Evaluation of satellite precipitation products for water allocation studies in the Sio-Malaba-Malakisi River Basin of East Africa

[1,3]Paul Omonge, [1]Karsten Schulz, [2,3]Luke Olang',[1]Mathew Herrnegger

[1]Institute for Hydrology and Water Management (HyWa), University of Natural Resources and life Sciences, Vienna

[2]Department of Biosystems and Environmental Engineering, Technical University of Kenya

[3]Centre for Integrated Water Resource Management, Technical University of Kenya, Nairobi, Kenya

Corresponding author email address: omonge.paul@gmail.com

Author Statement

This paper is a non-peer reviewed paper preprint submitted to EarthArXiv. It has been submitted for peer review to the Journal of Hydrology Regional Studies. Twitter @BOKU_HyWa

Abstract

Study region: Sio Malaba Malakisi river basin, East Africa. **Study Focus:** Poor rain-gauge density is a limitation to comprehensive hydrological studies in Sub-Saharan Africa. Consequently, Satellite precipitation products (SPPs) provide an alternative source of data for possible use in hydrological modelling. However, there is need to test their reliabilities across varied hydro-climatic and physiographic conditions to understand their applicability. In this study, we evaluated and compared the Tropical Rainfall Measuring Mission (TRMM-3B42 v7), Climate Hazards Group Infrared Precipitation (CHIRPS v2.0), Multi-Source Weighted-Ensemble Precipitation (MSWEP v2.2), Precipitation Estimation from Remotely Sensed Information using Artificial Neural Networks-Climate Data Record (PERSIANN-CDR) and Tropical Applications of Meteorology using Satellite (TAMSAT) against gauge observations, for possible use in water allocation studies. Furthermore, the Continuous Semi-distributed Runoff (COSERO) model was adapted using the SPPs and applied to generate discharges, which were cross-compared with observed discharges. **New Hydrological Insights for the region:** Our results indicate that the SPPs are able to detect seasonal rainfall patterns throughout the basin. At lower altitudes, the products overestimated rainfall events as indicated by the performance measures. The COSERO results indicate that PERSIANN-CDR and MSWEPv2.2 overcompensated and underestimated discharge throughout the basin. This could be attributed to differences in temporal dynamics of the products. In overall, seasonal trends captured by the SPPs can be used to support catchment management efforts in data scarce regions.

Keywords: Data-sparse regions, satellite precipitation products, COSERO model, rainfall estimations, Sio-Malaba-Malakisi river basin

1. INTRODUCTION

Rain gauges have been the mainstay of global rainfall measurements for a very long time. Inadequate rain gauge density, portends that the distribution of rainfalls cannot be well captured considering its high variability in time and space (Ouma et al. 2012; Ayanlade et al. 2018; Chen et al. 2018; Wolski et al. 2020). In Sub-Saharan Africa, the rain gauge density for a majority of the regions is often poor thereby limiting hydrological impact studies that require rainfall as a key forcing (Onyando et al. 2005; Liechti et al. 2012; Kimani et al. 2017). Moreover, where rain gauge networks exist, there are often issues related to the quality and accuracy of measurements, limited observations considering poor maintenance of the instruments, data-rights and hence sharing impediments (Habib et al. 2012; Maidement et al. 2014; Chwala & Kunstmann, 2019). Such bottlenecks motivate practicing hydrologists in such regions to look beyond the available ground instruments for alternative data sources to support impact analyses. More recently, there has become the need to combine new data collection and processing tools with a view to increase the reliability of such predictions (Olang and Fürst, 2010; Gebrechorkos et al. 2018; Zittis, 2018).

In ungauged basins, studies have shown that satellite rainfall products can be used as an alternative source of meteorological data important for river basin management studies (Blöschl et al. 2013; Maggioni & Massari, 2018; Belete et al. 2020; Brocca et al. 2020). In limited gauged basins, other studies have noted the need to corroborate the existing measurements with products derived from satellite based measurements, considering their extensive and dependable global coverage (Sooroshian et al. 2000; Jiang et al. 2018; Lakew et al. 2020). Consequently, the production and application of several satellite precipitation products (SPPs) has more recently seen an upward trend across many regions around the globe (Harris et al. 2014; Beck et al. 2017; Liu et al. 2017; Chen et al. 2018; Camici et al. 2020). While no single product can be said to be perfect for all conditions, there is the critical

need to test their utilities and reliabilities for applications across various hydro-climatic and physiographic conditions. Some studies already indicate that over complex topography and diverse climatic conditions, the uncertainties of the SPPs can be high (Rommily & Gebremichael, 2011; Dingman, 2015).

There has been increasing interest in the application of satellite precipitation products over East African regions of data scarcity (Näschen et al. 2018; Oduor et al. 2020; Pellarin et al. 2020). A majority of the studies have focused around the greater Lake Victoria drainage basin considering its economic significance (Habib et al. 2012; Williams et al. 2015; Awange, 2021). In relatively smaller transboundary basins however, not much has been done partly because of the varied national basin management plans that govern observed data sharing and acquisition, thereby limiting requisite validation of satellite based rainfall products. In a composite study over East Africa, Kimani et al. (2017) noted that most of the satellite precipitation products generally replicate the rainfall patterns but with observable differences when it comes to reproducing characteristics of orographic rainfall events. The precipitation products significantly overestimated rainfall amounts in the mountainous areas of East Africa. Similarly, the performance of Climate Hazards Group Infrared Precipitation with station data (CHIRPS) and Tropical Application of Meteorology using Satellite data (TAMSAT) over Eastern Africa, has been found to be varied and weaker in the coastal and mountainous regions (Dinku et al. 2018). Consequently, according to Li et al. (2009), the results for some of the products such as TRMM based Multi-Satellite Precipitation Analysis (TMPA), can be much improved by using a systematically bias-corrected TMPA rainfall data.

From literature, a majority of studies have largely focused on understanding the performance of TRMM and CHIRPS products in the region. This is partly because they are quasi-global products with relatively high spatial and temporal resolution, with uninterrupted and uniformly distributed precipitation estimates for the tropical region (Huffman et al. 2007;

Ngoma et al. 2021). Also, the focus of the studies has been on understanding drought and flood events, which are adequately captured by CHIRPS and TRMM products (Ayugi, et al. 2019). Few studies have focused on other products such as TAMSAT, the Multi-Source Weighted Ensemble Precipitation (MSWEP) and to some extent, the Precipitation Estimation from Remotely Sensed Information using Artificial Neural Networks-Climate Data Record (PERSIANN-CDR), which are considered relatively novel and improved over the years. This study incorporated such products, with a view to understand their performance and applicability for extended use in hydrological modelling in a mesoscale tropical river basin.

Several approaches have been employed to establish the reliability of satellite precipitation products as an alternative source of data (Knapp et al. 2011; Gebre & Ludwig, 2015; Belete et al. 2020). A common and most used approach is through comparison of derived georeferenced rainfall estimates with rain-gauge measurements through statistical measures such as the Root Mean Square Error (RMSE), Absolute Mean Error (AME), Correlation Coefficients (CC) and Bias (Moriasi et al. 2007; Thiemig et al. 2013). Another approach, which is also gaining presence lately, is the use of hydrological models. The model is first optimized using the available in-situ rainfall data, and subsequently used to simulate response of the catchment using the georeferenced SPPs (Stisen & Sandholt, 2010; Dessu & Melesse, 2012; Maggioni & Massari, 2018; Camici et al. 2020). The simulated discharges are then compared with observed discharges using objective functions such as Kling-Gupta Efficiency and Nash-Shutcliffe-Efficiency (Kling, 2002; Kling & Nachtnebel, 2009).

In this study, the two approaches were disparately tested with a view to better understand the satellite precipitation products for possible use in water allocation studies within the Sio-Malaba-Malakisi River Basin of East Africa. The statistical measures were first applied through direct comparison of the rainfall datasets and subsequently, the indirect model approach further used to understand the discharges variations in select areas with observed

data. The evaluation was important to discern products that can be used locally for enhanced catchment management in the transboundary River Basin spanning Western Kenya and Eastern Uganda in East Africa.

2. TOOLS AND METHODS

2.1. The Study Area

The study area is the Sio-Malaba-Malakisi river basin (SMMRB), a shared basin located between longitudes 33.7^{o} and 34.7^{o}E, and latitudes 0.1^{o} and 1.2^{o}N on the western Kenya border region with eastern Uganda. In total, 5,000 km^{2} are drained by three main rivers; the Sio river that flows from Mt. Elgon and into Lake Victoria in the south, Malakisi and Malaba rivers that flow into L. Kyoga and its wetlands in the south-west. The drainage pattern of the main stream, Sio River, is dendritic with a high drainage density. At its northern most point, the elevation of the SMMRB rises with Mt. Elgon to an altitude of 4320 meters above sea level (masl), while it merges with Lakes Victoria and Kyoga at an altitude of 1135 and 1033 masl respectively (Fig 1*).* The basin is nestled between these two striking topographic features, which play an important role in the hydrology of the region. Based on the two features, the area experiences two types of rainfall; orographic rainfall which occurs around Mt. Elgon and convectional rainfall near Lake Victoria. The rainfall pattern is normally bimodal, with long rains between March and June (MAM), and the short rains between September and November (SON). The average annual rainfall amounts in the basin vary according to the different climatic zones; the humid upstream region receives upwards of 2000 mm, the sub-humid mid-basin region receives 1511 mm per annum, while the semi-arid downstream area receives an average of 776 mm annually (Mugalavai et al. 2008). Temperatures in the basin are also highly influenced by orographic regimes due to Mt. Elgon. Mean maximum temperature is 28^{o} C in the low-lying areas and about 5^{o} around the slopes of Mt. Elgon. The vegetation and landcover comprise of high altitude moorland and forest, moist

savannah, dry savannah and farmlands. The area around the slopes of the mountain comprise of forests and the Mt. Elgon National Park and Forest Reserve, further there are grasslands, wetlands, woodland, shrubland and small scale cropland, irrigated and rain-fed (Dale, 1940; IUCN, 2005; WREM, 2008).

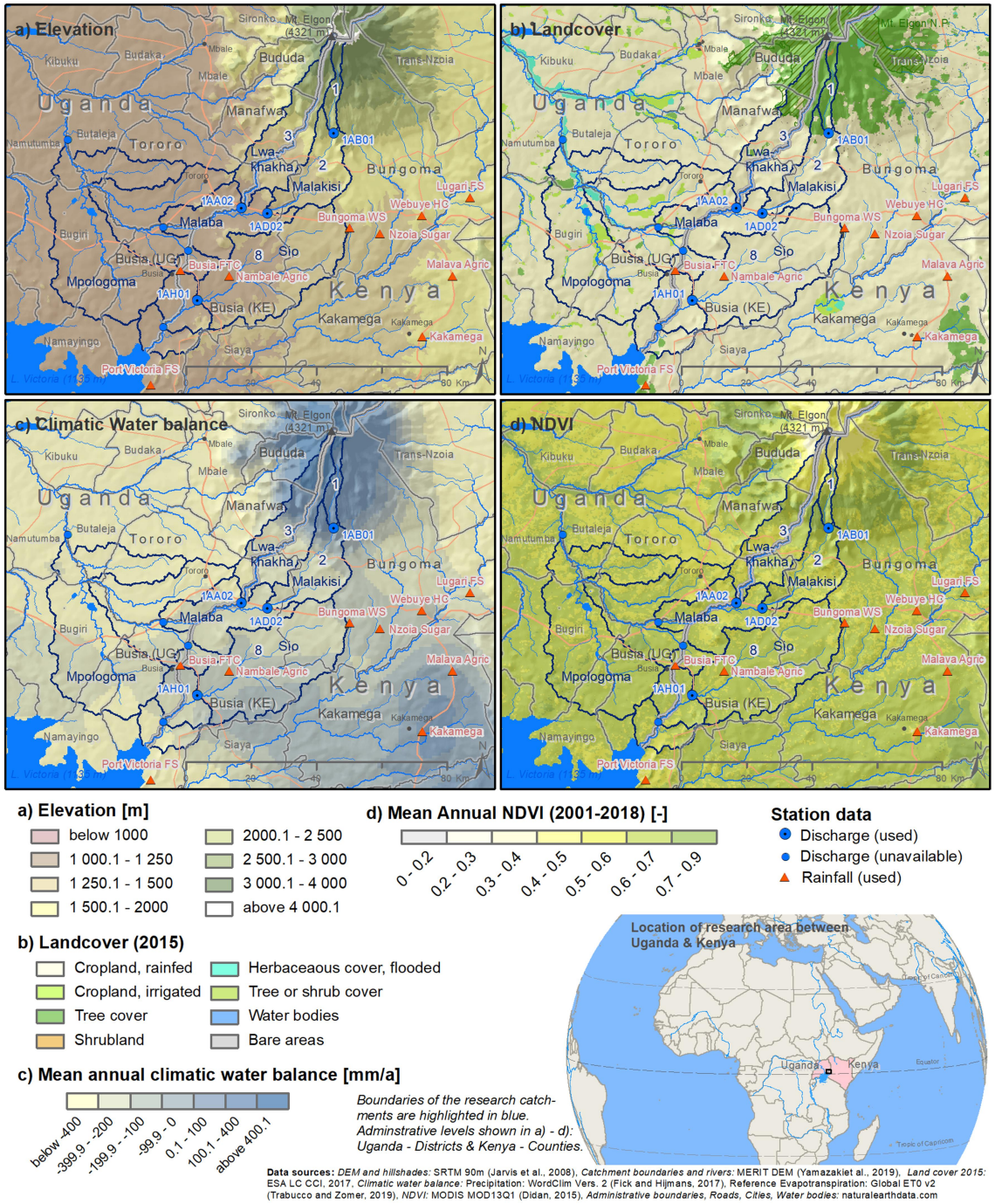

Figure 1: Map of the Sio-Malaba-Malakisi River basin showing the locations of hydro-meteorological stations against diverse backgrounds of Elevation, Landcover, Climatic water balance and NDVI.

2.2. Gauge-based datasets

Historical 10-day aggregates of observed precipitation time series was obtained from the Kenya Meteorological Department (KMD). A data quality assessment criterion was applied based on completeness of data (atleast 60% complete), value difference from, and its proximity to nearest neighbors as well as a check for systemic errors and extreme values. In this manner, only 9 out of 39 gauging stations were selected and a subset period of 1998-2016 chosen. The rainfall stations in the SMMRB tend to be located in areas with dense population, specifically in schools and government premises, they are also located in areas of intense agriculture as well as near forest stations (Fig 1). This acquired data, henceforth, served as the reference for the evaluation of downloaded satellite precipitation estimates. Additionally, daily streamflow records from hydrological stations in the SMMRB were acquired from the Water Regulatory Authority (WRA) in Kenya for the period 1981 to 2016 (Fig 1). The time series has extended periods of missing values due to measurement challenges, faulty instruments and limited reporting of measured values. Hydro-meteorological data acquisition in Uganda unfortunately proved to be an unresolvable challenge. *Table 1 and Table 2* provide a summary of the attributes of the rainfall and hydrological stations used in the study respectively.

Table 1: Kenya Meteorological Department Rainfall Stations used and their Attributes

Station ID	Station Name	Years Active	Lat	Lon	Elevation[m]	Equipment used
8934134	Bungoma	1966 - Present	0.5833	34.5666	1427	Tipping bucket
8934105	Busia	1957 - Present	0.4667	34.1000	1228	Symon's Rain gauge
8934096	Kakamega	1957 - Present	0.2833	34.7666	1524	Tipping bucket
8934016	Lugari FS	1932 - Present	0.6667	34.9000	1673	Symon's Rain gauge
8934061	Malava	1940 - Present	0.4500	34.8500	1646	Symon's Rain gauge
8934156	Nambale	1974 - Present	0.4500	34.2333	1234	Symon's Rain gauge
8934183	Nzoia Sugar	1980 - Present	0.5670	34.6500	1490	Tipping bucket
8934191	Port Victoria	1974 - Present	0.1500	34.0166	1236	Symon's Rain gauge
8934119	Webuye	1962 - Present	0.6166	34.7666	1562	Symon's Rain gauge

Table 2: Potential discharge measurement stations in the study area. Only data from Kenya were available for this study due to unresolvable data acquisition challenges in Uganda.

Sub-basin	Gauging Station	Area (km²)	Long	Lat	Elevation (masl)	Country
1.	1AB01	93	34.524	0.843	2109	KE
2.	1AD02	463	34.342	0.625	1189	KE
3.	1AA01	575	34.271	0.642	1144	KE
4.	82218	1524	34.051	0.585	1093	UG
5.	82226	83	34.120	0.520	1130	UG
6.	81269	1232	34.057	0.827	1150	UG
7.	82217	2868	33.790	0.827	1060	UG
8.	1AH01	1011	34.142	0.388	1163	KE

2.3. Satellite Precipitation Products (SPPs)

Satellite precipitation products are based on data derived from various sensors and satellites. They can also include other data sources such as ground radar, gauge networks or forecasts from model or reanalysis. In this study, five Satellite precipitation products were chosen because of their diversity, high spatial resolution, coverage domain, and periods of availability (Maidment et al. 2017). Additionally, the suitability of the products to capture precipitation patterns and extremes over a tropical region was considered. The product attributes are described in *Table 3*.

Table 3: Summary of the satellite precipitation products used in the study

Satellite Precipitation Product	Temporal extent	Temporal Res.	Spatial extent	Spatial Res.	Data Access sites
CHIRPS v2.0	1981 - Present	Daily	Land < 50°	0.05°	ftp://chg-ftpout.geog.ucsb.edu/pub/org/chg/products/CHIRPS-2.0/
PERSIANN-CDR	1983 - 2017	Daily	< 60°	0.25°	https://chrsdata.eng.uci.edu/
TRMM-3B42 v 7	1998 - Present	Daily	< 50°	0.25°	https://pmm.nasa.gov/data-access/downloads/trmm
MSWEP v2.2	1979 - 2017	3 hourly	Global	0.10°	www.gloh2o.org/
TAMSAT v2	1983 – 2018	10 daily	Africa	0.0375°	www.tamsat.org.uk/data/rfe/index.cgi

2.3.1 CHIRPv2

The CHIRPS dataset is a composite of five different data inputs that include; in situ rainfall measurements, pentadal precipitation climatology, quasi-global geostationary thermal infrared satellite observations from both the Climate Prediction Center infrared product and the National Climatic Data Center Infrared product (Knapp et al. 2011; Funk et al. 2015). It also utilizes the TRMM-3B42 product from NASA (Li et al. 2009), and atmospheric model rainfall fields from NOAA Climate Forecast System version 2 (Saha et al. 2010). The pentadal rainfall estimates are generated from satellite data based on cloud cover duration, which is based on regression models calibrated using TRMM. They are expressed as a percent of normal and multiplied by the corresponding precipitation climatology, station data is then blended with this data to produce CHIRPS (Dinku et al. 2018). Some of the Africa daily data has a finer spatial resolution of 0.25^{o} x 0.25^{o} to support land surface modeling activities. The final estimates are available in NetCDF, GeoTiff and Esri Bil formats (Funk et al. 2015).

2.3.2 TRMM 3B42v7

TRMM 3B42 v7 product combines passive microwave precipitation estimates from the Special Sensor Microwave Imager and Sounder, TRMM Microwave Imager, the Advanced Microwave Sounding Unit, the Microwave Humidity Sounder and the advanced Microwave Scanning Radiometer. The passive microwave data is first calibrated using the combined TRMM Microwave Imager and TRMM precipitation radar product and then used to calibrate geosynchronous infrared inputs. Rainfall estimates are freely available and have a temporal coverage of 1998 to 2015, with subsequent datasets provided by its successor, the Integrated Multi-satellite Retrievals for Global Precipitation Measurement, GPM IMERG (Huffman et al. 2007; Alazzy et al. 2017).

2.3.3 MSWEP v2.2

MSWEPv2 is a unique precipitation estimate that combines the advantages of gauge, satellite and reanalysis datasets to provide reliable precipitation estimates at a global scale. It optimally combines 76,747 gauge observations to determine precipitation estimates from WorldClim, Global Historical Climatology Network-Daily (GHCN-D), Global Summary of the Day (GSOD) and Global Precipitation Climatology Centre (GPCC). It merges these with non-gauge based sources such as infrared Gridded Satellite (GridSat), Global Satellite Mapping of Precipitation (GSMaP) and TRMM Multisatellite Precipitation Analysis (TMPA-3B42RT), and reanalysis products such as the Interim Reanalysis (ERA – interim), Center for Medium-Range Weather Forecasts (ECMWF) and the Japanese 55-year reanalysis (JRA-55) product (Beck et al. 2019). The processing involves gauge data quality control to remove erroneous zeros as is common in GSOD database, gauge-based assessment of satellite and reanalysis datasets, determination of long-term mean, precipitation frequency correction and dataset harmonization. The satellite and reanalysis precipitation datasets are then merged and a gauge correction scheme applied to the final product. The MSWEP v2 product is designed for hydrological modeling and to merge the highest quality precipitation data sources available as a function of time, scale and location (Nair & Indu, 2017; Beck et al. 2019).

2.3.4 TAMSATvs2

The dataset used in this study is derived from the TAMSAT version 2.0 dekadal (10 day) as a temporal timestep for rainfall estimates. The algorithm comprises two main data inputs, Meteosat thermal infrared (TIR) imagery from the European Organization for the Exploitation of Meteorological Satellites (EUMETSAT) and rain gauge measurements for calibration. The algorithm is a cloud indexing approach where the duration of cold cloud tops exceeding a certain temperature threshold acts as a proxy for rainfall (Maidment et al. 2014: 2017). For the

African region, the TAMSAT rainfall estimates have been validated using observed daily rain gauge measurements from five countries, that is; Mozambique, Niger, Nigeria, Uganda and Zambia (Tarnavsky et al. 2014).

2.3.5 PERSIANN-CDR

PERSIANN-CDR uses the archive of Gridded Satellite (GridSat-B1) Infrared data as an input to the PERSIANN model. The PERSIANN model algorithm combines IR and PMW information from multiple global geosynchrous satellites as the primary source of precipitation information. The algorithm uses an artificial neural network (ANN) model to extract cold-cloud pixels and neighboring features from GEO longwave IR images. It then associates variations in each pixel's brightness temperature to estimate the pixel's surface rainfall rate (Sorooshian et al. 2000; Ashouri et al. 2015). In order to eliminate PMW observations in the CDR product, the nonlinear parameters of the ANN model are trained and remain fixed when PERSIANN is used for retrospective estimation of rainfall rates using GridSat-B1 infrared window data. The resulting estimates are then bias corrected using the Global Precipitation Climatology Project (GPCP) 2.5^{o} monthly precipitation product (Liu et al. 2017). This product has been specifically developed for climate and variability studies.

2.4.Evaluation of Satellite products

Our main focus was to evaluate the performance of 5 satellite precipitation product estimates by comparing them to station observations across the SMMRB. The comparison is done at both the monthly and annual time steps. The products are then used as input in a hydrological model to further compare their performance with observed discharge in an indirect comparison approach. This section describes the methodology applied.

2.4.1 The Approach employed

Point values from the pixels of each satellite product was georeferenced to gauge location and extracted from the raster files downloaded from data access sites (Table 3). A point-based comparison between the rain gauge stations and the extracted satellite pixel value was used to evaluate performance of the products in this study. The satellite derived rainfall estimates and the observed rain gauge data were aggregated for the period 1998-2016, since this is the period that coincides with the availability of relatively continuous rainfall gauge measurements in the area. To allow for comparison of the products with the rain gauge scales, the Satellite estimates were aggregated to monthly and annual temporal resolutions. The analysis then focused on the comparison of individual gauge observations versus satellite estimates as done by Alazzy et al. (2017) and Lakew et al. (2020). To guide the comparative analysis, two different analytical approaches were applied: the continuous statistical measurement and a hydrological evaluation using the COSERO Hydrological model.

2.4.2 Statistical measurements

Various statistical measurements were applied to corroborate the performance of satellite precipitation products with gauged observations (Table 4). In this regard, the following validation measurements were used; correlation coefficient (CC), mean error (ME), mean absolute error (MAE), root-mean-square error (RMSE), and Percent bias (R_{bias}). These are calculated, as shown in *Table 4* Eq. (1) to Eq. (5), respectively (Moriasi et al. 2007; Thiemig et al. 2013).

Table 4: Continuous statistical measurements used in the study

Statistical Measure	Formula	Best Value	Equation
Mean Error (ME)	$\frac{\sum_{i=1}^{n}(P_{est,i}-P_{obs,i})}{n}$	0	Eq.(1)
Mean Absolute Error (MAE)	$\frac{\sum_{i=1}^{n}\lvert(P_{est,i}-P_{obs,i})\rvert}{n}$	0	Eq.(2)
Coefficient of Correlation (CC)	$\frac{\sum_{i=1}^{n}(\bar{P}_{obs,i}-P_{obs,i})(P_{est,i}-\bar{P}_{est,i})}{\sqrt{\sum_{i=1}^{n}(\bar{P}_{obs,i}-P_{obs,i})^2}\sqrt{\sum_{i=1}^{n}((P_{est,i}-\bar{P}_{est,i})^2}}$	1:1 line	Eq.(3)
Root Mean Square Error (RMSE)	$\sqrt{\frac{\sum_{i=1}^{n}(P_{est,i}-P_{obs,i})^2}{n}}$	0	Eq.(4)
Percent Bias (P_{bias})	$\frac{\sum_{i=1}^{n}P_{est,i}-\sum_{i=1}^{n}P_{obs,i}}{\sum_{i=1}^{n}P_{obs,i}}\ x\ 100$	0	Eq.(5)

Where $\boldsymbol{P_{est}}$ *are the satellite precipitation estimates and* $\boldsymbol{P_{obs}}$ *is the observed rain gauge precipitation, over bar is the mean and n is the number of samples considered.*

2.4.3 Hydrological Evaluation

The hydrological simulations were performed using the conceptual rainfall-runoff model COSERO (COntinuous SEmidistributed RunOff Model; Eder et al. 2005; Stanzel et al. 2008; Kling and Nachtnebel 2009; Kling et al. 2015; Herrnegger et al. 2018, 2015, 2012; Wesemann et al. 2018), which has a construct that is comparable to the HBV model (Hydrologiska Byråns Vattenbalansavdelning model, Bergström, 1995).

The model was developed at the University of Natural Resources and Life Sciences, Vienna (BOKU) and evolved from a model structure that was originally developed for real-time runoff forecasting for the Enns River in Austria (Nachtnebel et al. 1993). Since then, substantial improvements have been incorporated into the model, e.g. for the application of COSERO to water balance studies, real-time flood forecasting systems, distributed routing issues, or for implementing new optimization methods (Herrnegger et al. 2012, 2018). COSERO accounts for actual evapotranspiration, interception storage, soil water storage, separation of runoff into different flow components and routing by means of a cascade of

linear and non-linear reservoirs. A detailed description of the model, including some previous applications and model equations, can be found in Kling et al. (2015).

Given the limited availability of spatially distributed data in the SMMRB, the model was setup in a lumped manner, with the SMMRB being divided into ten sub-catchments (Fig. 1, Table 1). The Shuttle Radar Topography Mission digital elevation model (SRTM30 DEM; Jarvis et al. 2008; Faramarzi et al. 2015) was used for sub-basin and stream delineation. Sub-basin outlets consider gauge station locations, but also important physical characteristics, e.g. the confluence of important tributaries. Land use maps for developing mean land use classes were obtained from the European Space Agency Land cover classification map of Africa (ESA, https://www.esa.int/ESA_Multimedia/Images/2017/10/African_land_cover/) which has a resolution of 20m and distinguishes 10 land use classes for Africa and 10 classes for the SMMRB. Dominant land use and vegetation were considered to characterize each sub-basin in this study.

The acquired Satellite precipitation estimates were used as rainfall inputs into the COSERO model to predict possible catchment runoff responses. For this study, Climatic Research Unit Time series (CRU TS v.4.01) global gridded data from the University of East Anglia (Harris et al. 2014) for potential evapotranspiration was used. The simulation results were compared with historical measured records at 3 gauging stations. The observed records for gauging station 1AB01 had many errors and since it pours into gauging station 1AD02, the later stations' record were used instead. The simulated monthly discharges were compared with the measured discharge acquired from the WRA.

2.4.4 Simulation periods and parameter evaluation

The streamflow simulation was done for the period 1983 to 2016 with a spin-up period of two-years (1981 and 1982) to equilibrate the system states and to mitigate for unknown initial conditions. The model was calibrated for the period 1983 to 2002 (25 years) and validated for

the period 2003 to 2016 (13 years). The COSERO model was run with monthly timesteps (Wesemann et al. 2018; Mehdi et al. 2021). The Shuffle Complex Evolution (SCE) optimization algorithm method was applied for the calibration of the model. The SCE optimization method was chosen over other optimization methods such as Monte Carlo, Rosenbrock and DDS because it combines four crucial concepts desirable in a conceptual watershed hydrological model calibration; (i) systemic evolution of a complex of points across the parameter space (iii) competitive evolution (iv) complex shuffling. These elements make the SCE method effective, robust, flexible and efficient (Duan et al. 1994; Schulz, Herrnegger & Wesemann, 2016; Kratzert et al. 2018) A total of 13 parameters were selected for calibration in the SMMRB. The calibration procedure exposed the poor quality of observed discharge data with the many gaps weakening the performance of certain products (Fig 2). To evaluate the model performance, the following objective functions are applied.

Table 5: Objective criteria used in the model performance evaluation

Objective criteria	Formula	Best value	Equation
NSE - Nash-Sutcliffe-Efficiency Where: n - Total number of time-steps $Q_{sim,t}$ /$Q_{obs,t}$ - Simulated & Observed runoff at time step t $\overline{Q_{obs}}$ - Mean of observed runoff	$1-\frac{\sum_{t=1}^{n}(Q_{sim,t}-Q_{obs,t})^2}{\sum_{t=1}^{n}(Q_{obs,t}-\bar{Q}_{obs})^2}$	1	Eq.(6)
Pearson's correlation	$r=\frac{\sum_{i=1}^{n}(\bar{P}_{obs,i}-P_{obs,i})(P_{est,i}-\bar{P}_{est,i})}{\sqrt{\sum_{i=1}^{n}(\bar{P}_{obs,i}-P_{obs,i})^2}\sqrt{\sum_{i=1}^{n}((P_{est,i}-\bar{P}_{est,i})^2}}$	1	Eq.(7)
Kling-Gupta Efficiency (KGE) *Where*: σ - Standard deviation $\overline{Q}_{sim,t}$- $\overline{Q}_{obs,t}$ - Mean of simulated/observed runoff	$1-\sqrt{(r-1)^2+\left(\frac{\sigma_{sim}}{\sigma_{obs}}-1\right)^2+\left(\frac{\overline{Q_{sim,t}}}{\overline{Q_{obs,t}}}-1\right)^2}$	1	Eq.(8)
Mean Square Error	$MSE=\frac{1}{n}\sum_{i=1}^{n}(x_{S,t}-x_{O,t})^2$	0	Eq.(9)

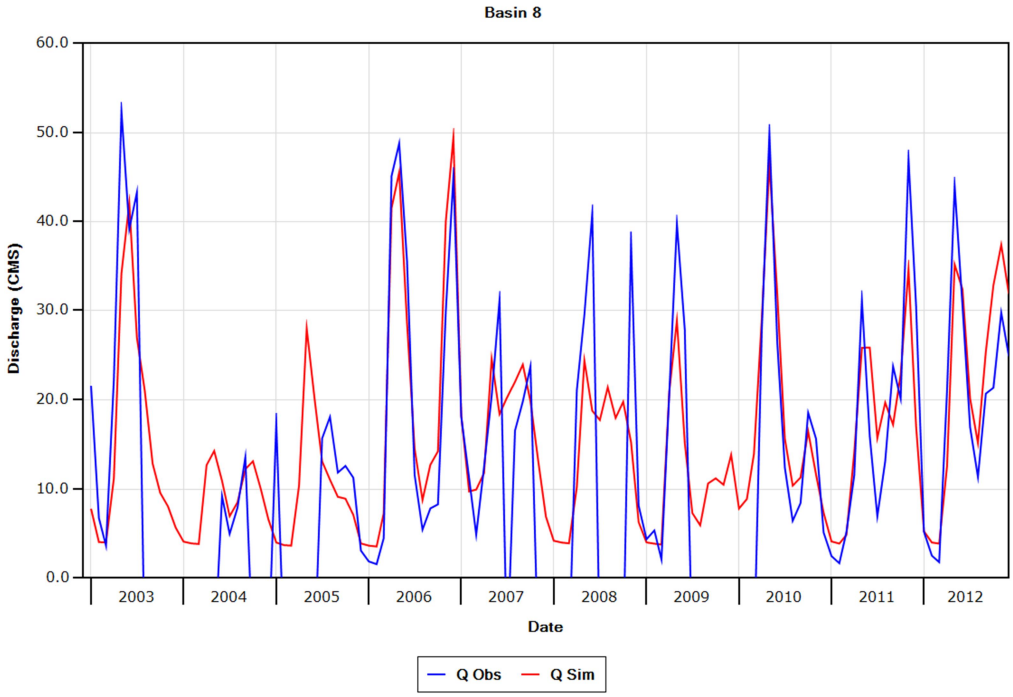

Figure 2*:* Simulated and observed discharge with CHIRPSv2 product for Basin 8 for the Validation period Jan 2003 to Dec 2012

3 RESULTS

3.1 Station distribution

To get a better understanding of the performance of the satellite precipitation estimates against the observed precipitation, we first briefly explore the status of the observed precipitation and the station distribution. The observed precipitation indicates a mixed but related rainfall distribution across the basin. There are clear similarities on rainfall amounts and distribution among stations that are closer to each other and lie in a relatively similar altitude (Table 1, Fig 1). For example, Busia (1228 masl) is closer to Nambale (1234 masl), Bungoma (1427 masl) is closer to Nzoia (1490 masl) and Webuye (1562 masl) is closer to Lugari (1673 masl), hence the pairs depict almost similar rainfall distribution (Fig 3). Busia and Nambale lie in the middle of the basin and depict larger distribution of rainfall, which could be an effect of their equidistant from two key natural features, Mt. Elgon and Lake Victoria, whose different

rainfall regimes (orographic and convectional rainfall regimes) contribute to increased rainfall amounts in the middle of the basin.

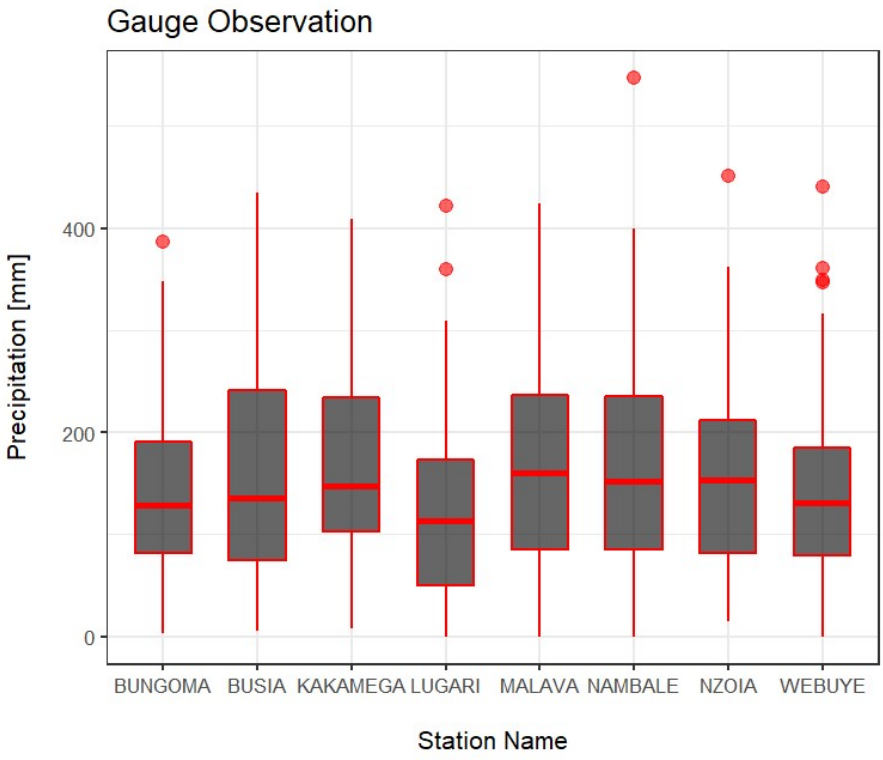

Figure 3: Boxplot of mean monthly station rainfall distribution across the SMMRB (1998 – 2012)

3.2 Evaluation of Satellite precipitation products performance

3.2.1 Performance against station observations – Monthly time scale

The performance of the satellite products in comparison to the station observations are evaluated and compared over the SMMRB. The observed low rainfall amounts at the lower altitude region, is in contrast to the high amounts in the rest of the basin (Fig 4 & Table 1). This can be attributed to the fact that the rest of the basin receives both orographic and convectional rainfall events with increasing amounts towards Mt. Elgon (Kansiime et al. 2013). Consequently, all the SPPs overestimated the rainfall amounts in this area - which normally experiences convectional type of rainfall. At a monthly time scale, CHIRPSv2 and TAMSATv2 perform best with a correlation coefficient of 0.75 each, followed by

MSWEPv2.2 at 0.72, while TRMM3B42 and CDR produced a CC performance of 0.60 and 0.58 respectively (Table 6). The better performance by CHIRPSv2, TAMSATv2 and MSWEPv2.2 may be because the estimates are bias corrected using gauge measurements hence improving the quality of the final product. Apart from MSWEPv2.2, all the products overestimate rainfall at PORTVICTORIA.FS, which is the station that is closest to Lake Victoria. MSWEPv2.2 performed similar to the observed measurements while slightly underestimating rainfall peaks in the rainy seasons (by upto 3%). At LUGARI, the station at the highest altitude among the stations evaluated, TRMM overestimated rainfall by 19% followed closely by CHIRPSv2 at 17%. At the same time, MSWEPv2.2 underestimated by 7%. TAMSAT performed closest to gauge measurement with only 5% overestimation. The best Pbias performance was observed in MSWEPv2.2 and CHIRPSv2 products; at 4% and 14% respectively. PERSIANN-CDR posted the poorest Pbias performance at 59% (Table 6).

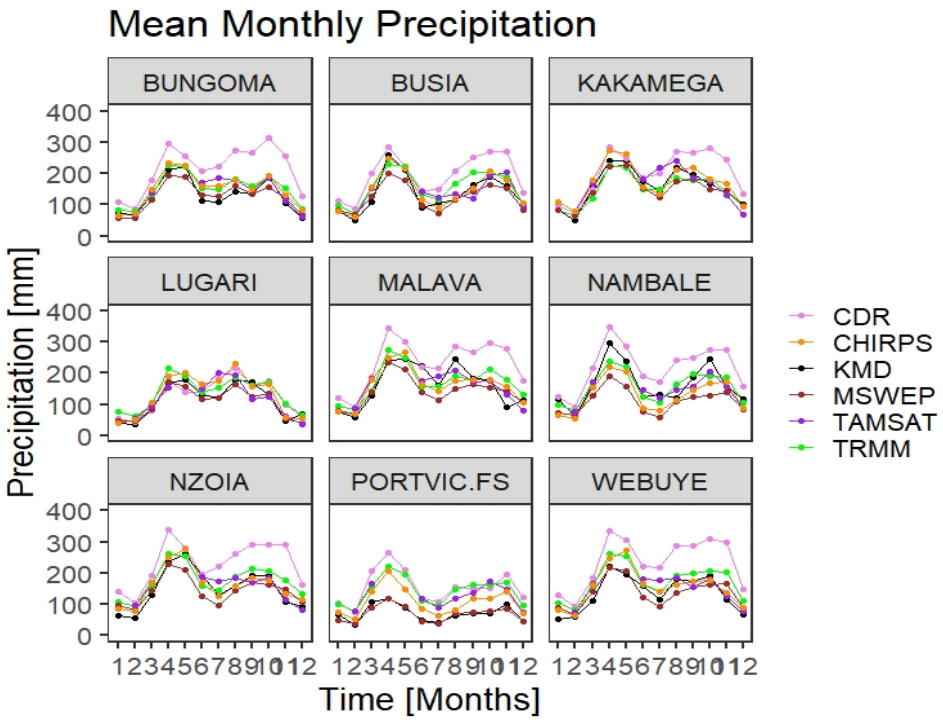

Figure 4*:* Long Term Mean Monthly comparison with station data (KMD = gauge)

Table 6: Validation statistics for mean monthly rainfall products in comparison to station data (CC-Correlation coefficient; ME – Mean Error; P_{Bias} – Percent Bias; RMSE – Root Mean Squared Error)

Dataset	CC	ME (mm)	P_{Bias}	RMSE(mm)
CDR	0.58	65.53	59	79.16
CHIRPS	0.75	10.32	-14	31.46
MSWEP	0.72	-13.45	4	33.06
TRMM-3B42	0.60	20.76	-28	39.41
TAMSAT	0.75	15.35	-21	35.85

The scatter-plot in Fig 5 presents the evaluation of the five satellite precipitation products with rain gauge measurements at the monthly time-scale. All the products correctly represent the spatial distribution of rainfall. However, PERSIANN-CDR has a wider scatter than the other products, it also tends to overestimate station rainfall amounts. MSWEPv2.2 underestimates some of the rainfall amounts. CHIRPSv2, MSWEPv2.2 and TAMSATv2 rainfall fields have less scatter beyond 300mm per month. In addition, the differences in monthly average precipitation amount enlarges as the precipitation amount increases.

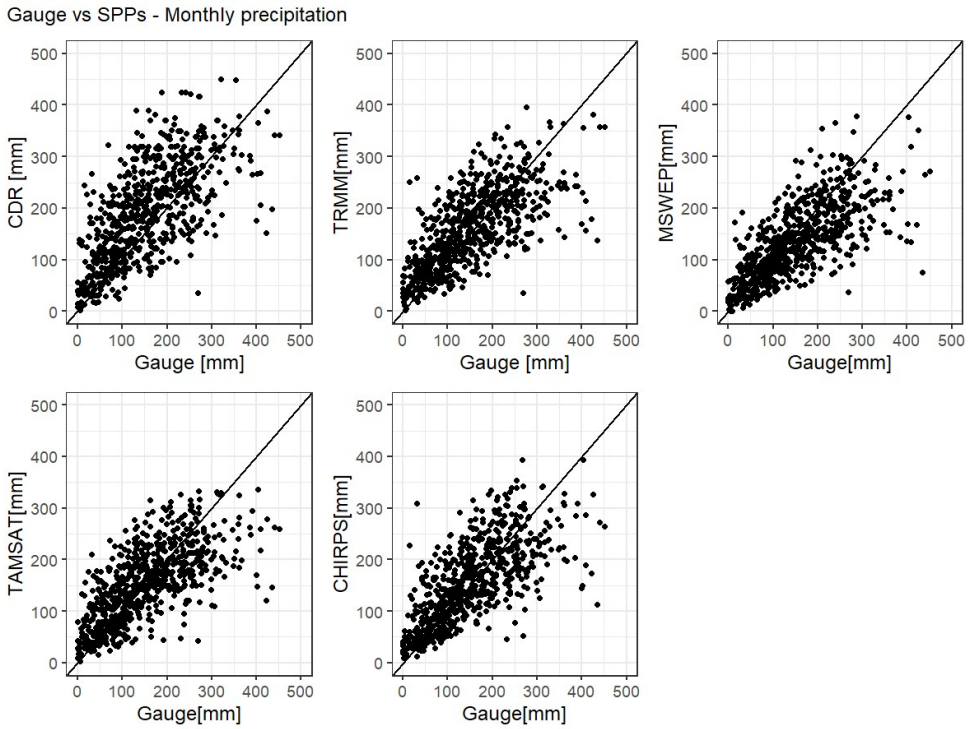

Figure 5: Scatter-plot comparison of SPPs and gauge precipitation on a monthly average timescale (mm/month) 1998 – 2012

In a correlation matrix (Table 7), all the products show a positive correlation with gauge measurements. However, the strongest relationship is with CHIRPSv2 (0.72) followed by products such as TRMM3B42, MSWEPv2.2 and TAMSATv2 which all registered a correlation coefficient of 0.70. On the other hand, PERSIANN-CDR registered the lowest performance at 0.59. In general, the pairs of MSWEPv2.2 and TRMM3B42, MSWEPv2.2 and CHIRPSv2 have a strong correlation with each other (0.89) at the monthly scale.

Table 7: Correlation matrix SPPs vs Gauge

GAUGE	1.00					
CDR	0.59	1.00				
TRMM	0.70	0.80	1.00			
MSWEP	0.70	0.71	0.89	1.00		
TAMSAT	0.70	0.74	0.80	0.77	1.00	
CHIRPS	0.72	0.73	0.86	0.89	0.86	1.00
	GAUGE	CDR	TRMM	MSWEP	TAMSAT	CHIRPS

3.2.2 Evaluation at an annual time-scale

At the annual scale, TRMM-3B42 underestimates the rainfall events with a correlation coefficient of 0.60 and a Pbias of 36%, while PERSIANN-CDR overestimates the rainfall events with a correlation coefficient of 0.76 and a Pbias of 62%. (Fig 6, Table 8). On the other hand, CHIRPSv2, TAMSATv2 and MSWEPv2.2 register good performances at this time-step compared to gauge measurements. However, when we consider the Pbias, the root mean square error and the correlation coefficient, TAMSATv2 and MSWEPv2.2 slightly outperform CHIRPSv2.2 and TRMM-3B42.

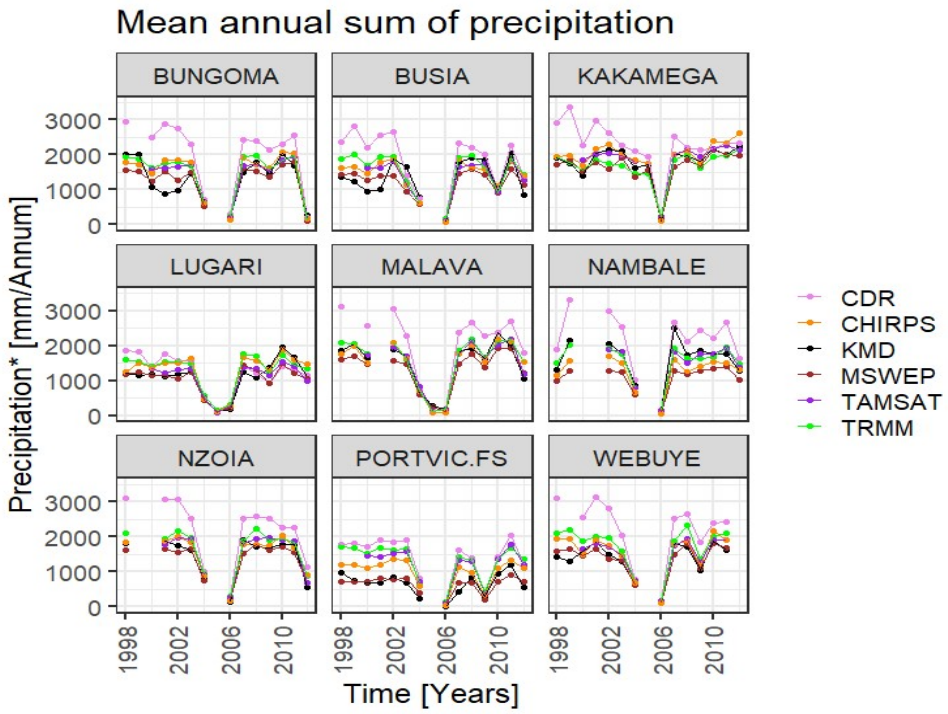

Figure 6: Long term mean annual comparison with station (KMD) data (1998-2012)

Table 8: Validation statistics for long-term mean annual performance of SPPs (1998 – 2012)

Dataset	CC	ME	P_{Bias}	RMSE
CDR	0.76	624.22	62	824.56
CHIRPS	0.74	107.73	-16	314.87
MSWEP	0.77	-128.42	2	296.84
TRMM-3B42	0.60	193.87	-36	394.09
TAMSAT	0.79	119.58	-27	307.99

In the scatter-plots of the annual sums (Fig 7), PERSIANN-CDR overestimates most of the rainfall amounts with a wider scatter compared to the other products. TRMM3B42, TAMSATv2 and CHIRPSv2 also overestimate rainfall amounts but with less scatter than PERSIANN-CDR. However, it is also evident that MSWEPv2.2 tends to underestimates rainfall at the annual time-step similar to the underestimation seen in the monthly evaluation.

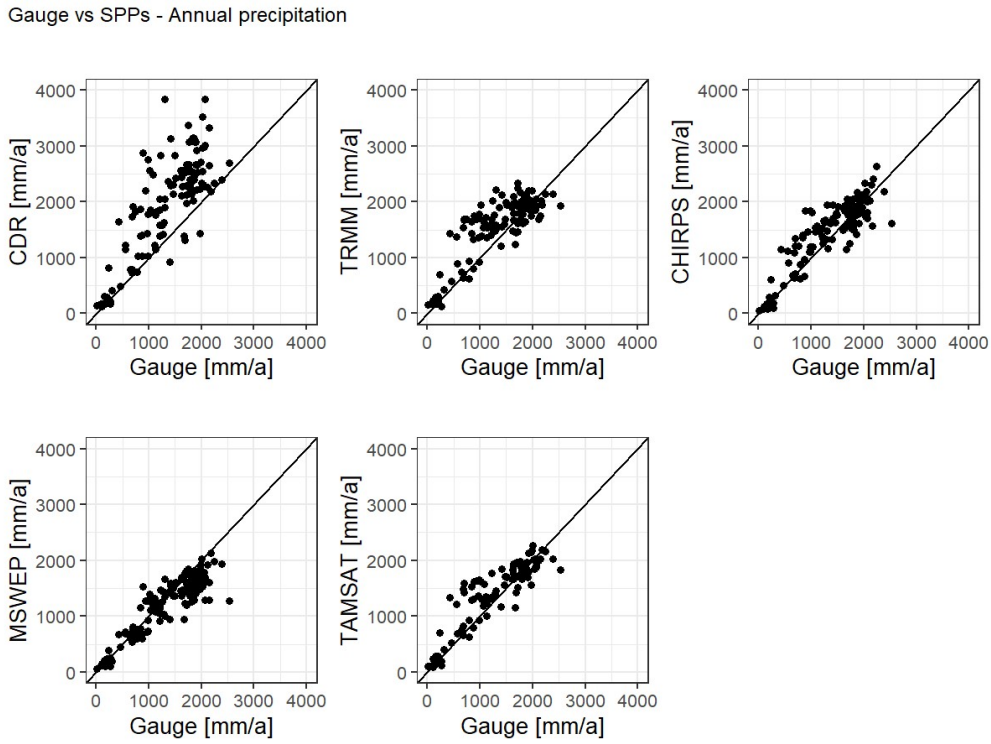

Figure 7*:* Scatter plot comparison of satellite and Gauge precipitation at an annual scale (1998 -2012)

3.3 Indirect evaluation with a hydrological model

3.3.1 Water balance evaluation

The different satellite precipitation products were used as input into the COSERO model to generate discharge. The simulations were then compared against gauge measurements as a performance measure. A summary of the overall statistical performance is provided in the appendix of this article (Appendix Tables A.1 and A.2). In basin 2, which is characterized by a mountainous terrain, the performance indicates overcompensation by the model for most of the generated discharges. This can be attributed to both the quality of observed discharge data at 1AD02 as well as the varying capability of some of the satellite products to retrieve rainfall events in mountainous regions (Dinku et al. 2011; Chen et al. 2013). The simulated discharge is much higher in CHIRPSv2 and MSWEPv2.2, while it is lowest in TRMM3B42. This is consistent with Li et al. (2009) and Kimani et al. (2017), who observe that TRMM3B42 underperforms in mountainous terrains. Generally, simulated discharge exceeds the observed

discharge. In basin 3, the water balance performance by all the products improves significantly compared to basin 2. TRMM3B42 and PERSIANN-CDR performs best while MSWEPv2.2 performs poorly compared to the other products. In basin 8, there is further deterioration in the water balance performance by all the products, with the best performance posted by MSWEPv2.2 and the worst by PERSIANN-CDR. However, the difference in performance by all the products is marginal in this basin as is the case in the previous 2 basins (Fig 8, 9 and 10).

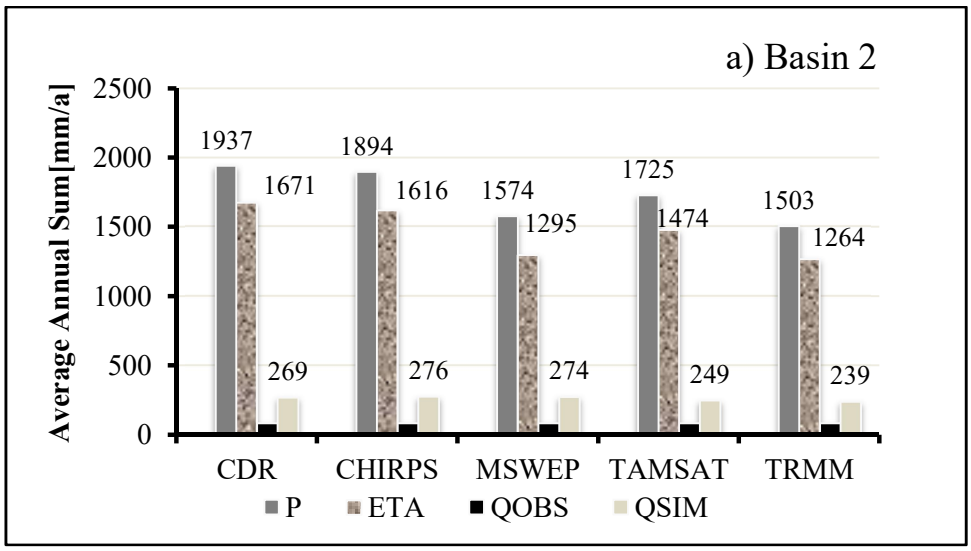

Figure 8: Simulated Water Balance components and observed discharge for the SPPs in basin 2

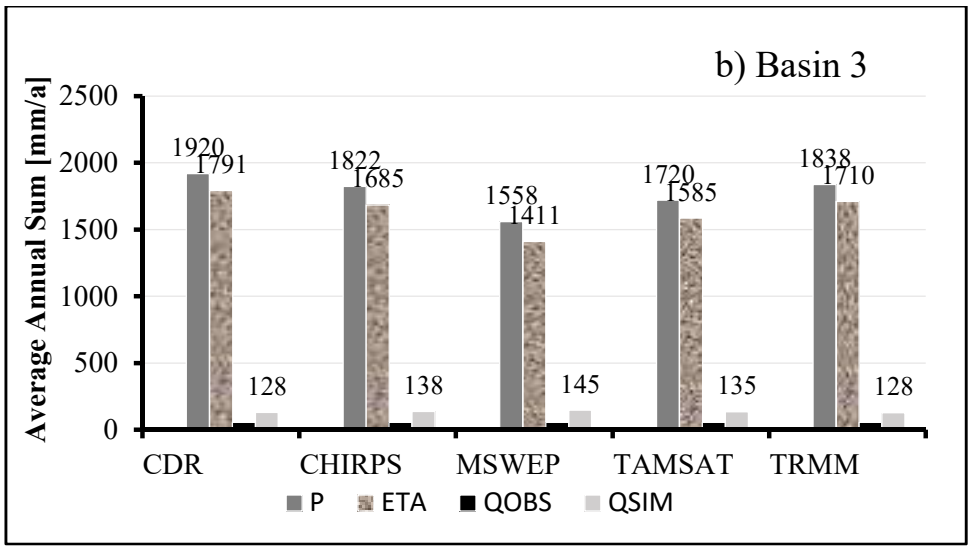

Figure 9: Simulated Water Balance components and observed discharge for the SPPs in basin 3

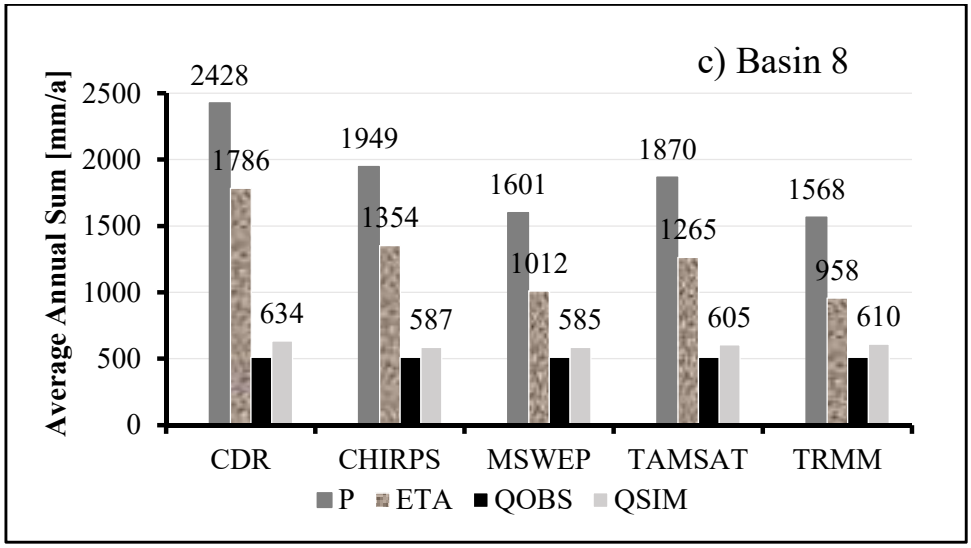

Figure 10: Simulated Water Balance components and observed discharge for the SPPs in basin 8

3.3.2 Actual Evapotranspiration

Actual Evaporation estimates of over 1000 mm or 66% of the rainfall is not unusual in the study area (Piper, Plinston & Sutcliffe, 1986; Alemayehu et al. 2017). In this regard, the ETA performance differs with the simulations with different SPPs. However, the real ETA value for this basin is unknown since no measurements exist. PERSIANN-CDR had the highest ETA value of over 1500 mm/a for all the basins, while MSWEPv2.2 registered a value closest to estimated area average of 1000mm/a in all the basins. Three products, CHIRPSv2, MSWEPv2 and TAMSATv2 all registered overlapping values in basin 8, while only TAMSATv2 in basin 8 and PERSIANN-CDR in basin 3 registered overlapping or near overlapping values during the calibration and validation process (Fig 11, 12 and 13).

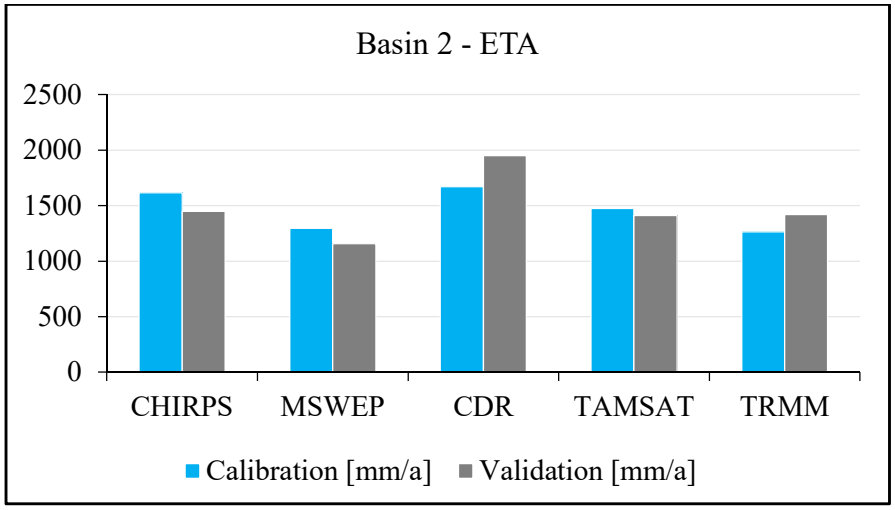

Figure 11: Simulated actual evapotranspiration - Basin 2

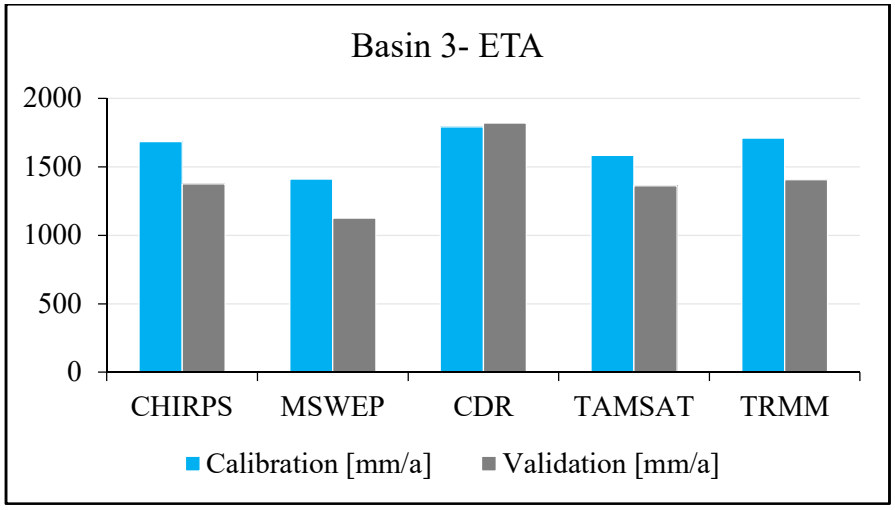

Figure 12: Simulated actual evapotranspiration - Basin 3

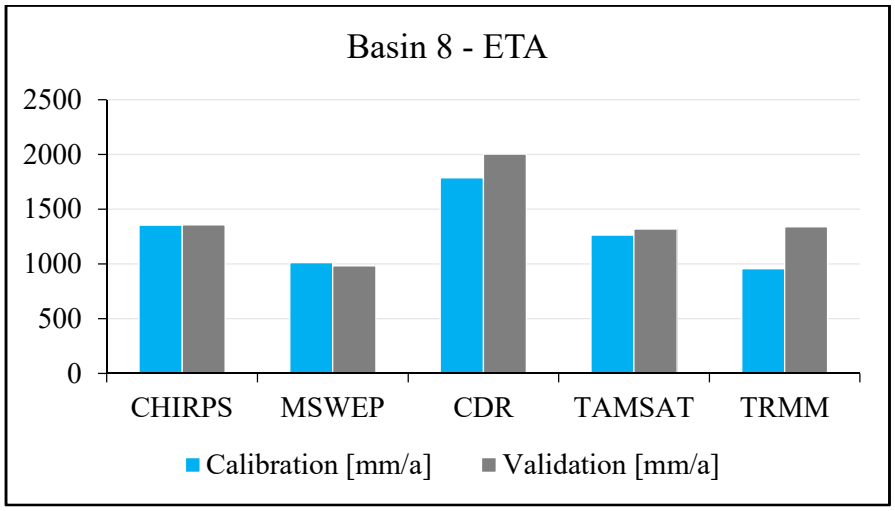

Figure 13: Simulated actual evapotranspiration - Basin 8

3.2.3 Bias performance evaluation

The various products registered varied bias performances in different basins. However, the magnitudes of bias often fell below 0.35 which indicates better performance by the model. However, in basin 8, PERSIANN-CDR registers an extreme bias of 10 in the validation process, an indication of deterioration in model performance (Fig 16). In basin 2, MSWEPv2 exhibits a better bias of less than 0.05 in both calibration and validation procedures. TRMM-3B42 and TAMSATv2 both register a negative bias of 0.15 in the same basin (Fig 14). In basin 3, MSWEPv2.2 registers the strongest bias at 0.32 hence the weakest performance of the 5 products. The product with the best bias at basin 3 is TRMM3B42 with a negative bias below 0.05 at both the calibration and validation process (Fig 15).

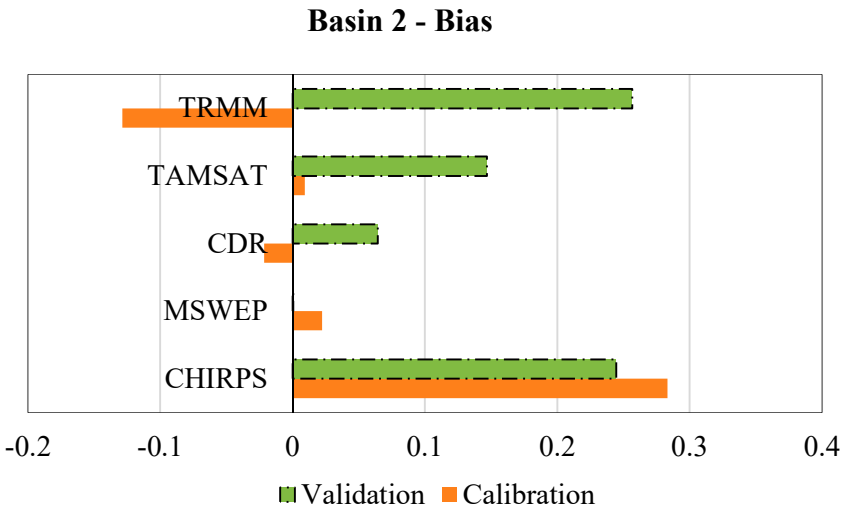

Figure 14: Simulated Bias Performance - Basin 2

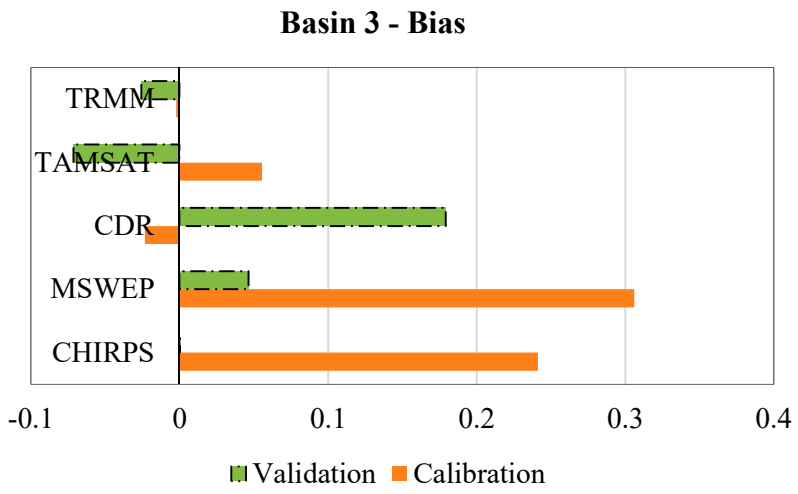

Figure 15: Simulated Bias performance - Basin 3

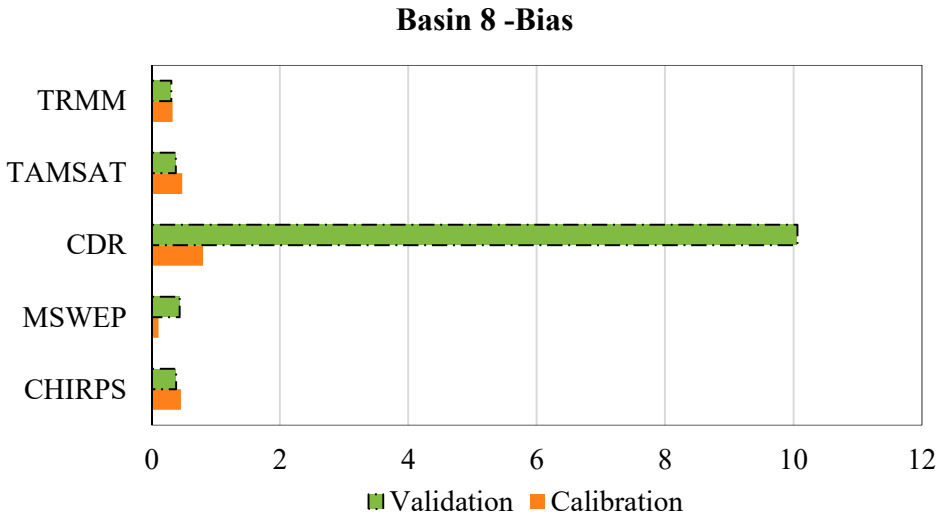

Figure 16: Simulated Bias performance - Basin 8

3.2.4 NSE performance evaluation

The NSE performance from basin 8 indicate a performance of 0.56 to 0.73 by all the products except PERSIANN-CDR which posted an NSE value of -1.19 (Fig 17). However, the NSE performance was poor for both basins 2 and 3 (Fig 17, 18). For instance, the performance for the products at basin 3 only range from 0.31 to 0.38, with TAMSATv2 posting the lowest value at 0.31, while MSWEPv2.2 posted the highest at 0.38. At basin 2, MSWEPv2.2

performed the lowest at NSE value of 0.23 while CHIRPSv2 and TRMM-3B42 all presented similar NSE values of 0.51. To better understand the performance of the products in the SMMRB, we can deduce NSE performance from basin 8 (Fig 19), which had fairly complete observed discharge data in the study area. In that regard, MSWEPv2.2, CHIRPSv2, TRMM-3B42 and TAMSATv2 exhibit decreasing performances in that order respectively.

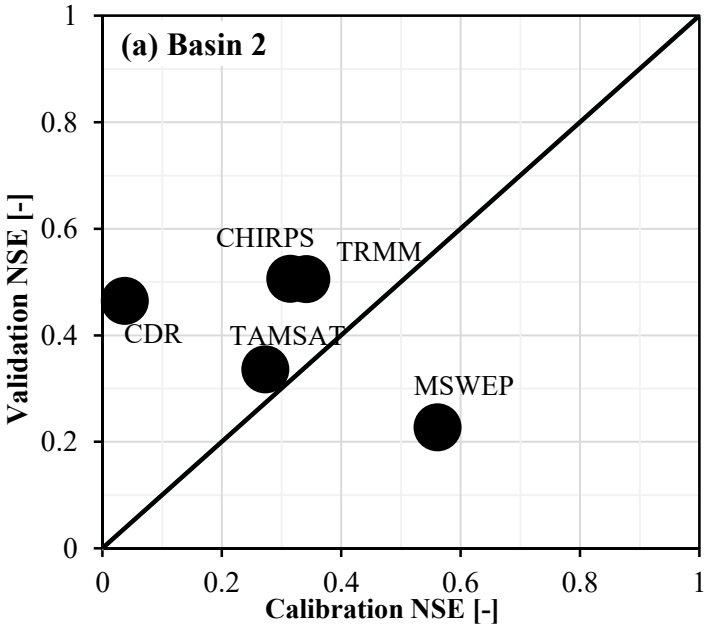

Figure 17: NSE Performance for Basin 2

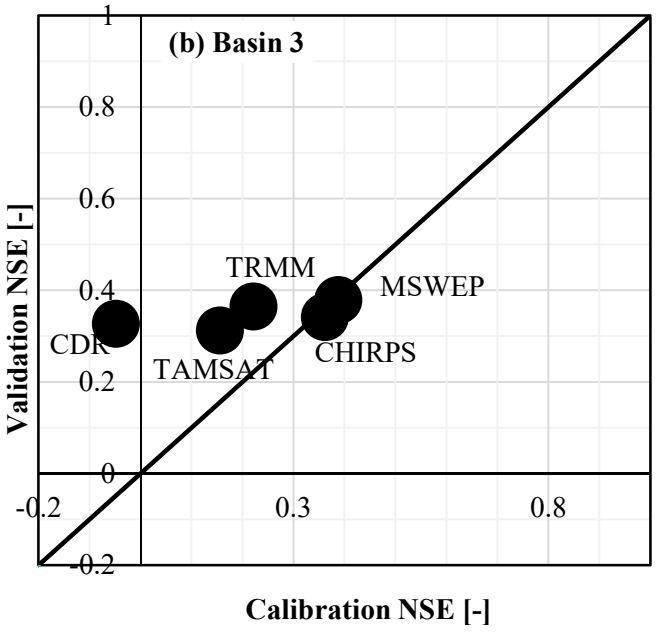

Figure 18: NSE performance for Basin 3

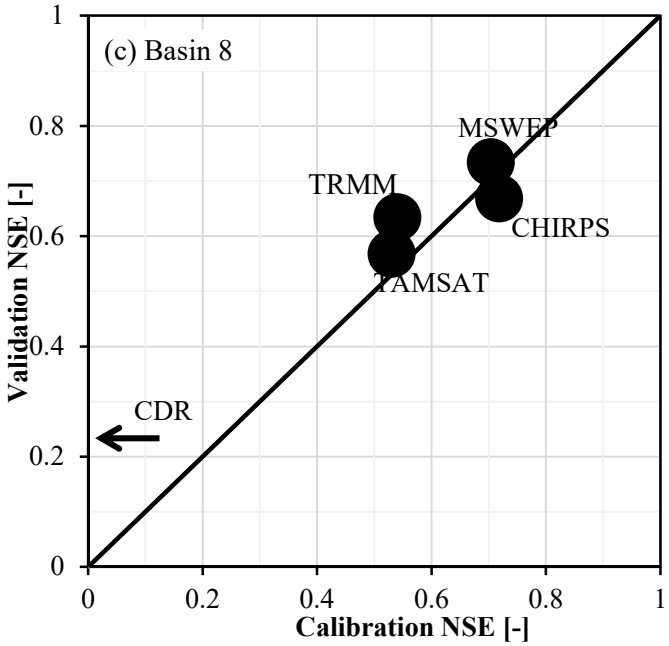

Figure 19: NSE performance for Basin 8

4 DISCUSSION

The objective of this study was to compare the performance of different satellite precipitation products with gauged data and to determine their quality as inputs to a hydrological model in a data sparse tropical basin. First, we focused on the comparative performance of each satellite product within the Sio-Malaba-Malakisi river basin (SMMRB) basin. Afterwards, we tested the usefulness and suitability of each product in driving hydrological simulations with the COSERO model, on a monthly timestep. In our instance, the model was calibrated using available discharge data from three sub-basins. Calibrated parameters reflect any errors or inconsistencies in the gauge data such as inadequate spatial representation or the manner in which the gauge data was used to obtain sub-basin average rainfall inputs.

The overall performance by the products is acceptable because a majority are able to reproduce the station measurements with varying degrees of accuracy. The average bias of 0.25 and an average coefficient of correlation of 0.68 indicate a fair performance by the products to replicate observed measurements. The products are also able to correctly capture the seasonal rainfall patterns in the basin. However, certain products such as PERSIANN-

CDR (Bias = 0.59) and TRMM3B42 (Bias = 0.28) had obvious biased performances that over-estimated and underestimated rainfall significantly. The performance of TRMM-3B42 was highly influenced by topography as seen by the poor performance in stations like Kakamega that experience high amounts of rain. Consequently, the evaluation results was found to echo those found by Ouma et al. (2012) in the neighboring Nzoia river basin, which proposed adjustments or a correction index for the use of products such as TRMM3B42 in the area based on temporal scales, topography and rainfall season. As observed over the Blue Nile Basin by Belete et al. (2020), CHIRPSv2 and TAMSATv2 performed best by replicating the highest volume of precipitation throughout the two rainy seasons as captured by station measurements. This can be attributed to the fact that they include gauge observations in calibrating acquired rainfall estimates (Maidment et al. 2014, Funk et al. 2015).

As for the varying performance of SPPs in the COSERO hydrological model in the area, two observations are evident. The quality of the measured hydro-meteorological data used cannot be guaranteed, and two, that the results obtained here reflect those obtained from previous studies with other models (Coron et al. 2012, Alfieri et al. 2013), which conclude that the reliability of certain model simulations such as COSERO and MORDOR6 decreases from the humid European basins, to the hydrologically heterogeneous African basins. For example, in Basin 8, the most significant Kling-Gupta-Efficiency (KGE) performance was registered by MSWEPv2.2 (0.77) and CHIRPSv2 (0.75), while the poorest performance was by PERSIANN-CDR (0.37). This varied performance is a clear indication of the challenge of data acquisition and how this impacts hydrological studies. The bias performance of TRMM-3B42 (0.31) was better against TAMSATv2 (0.38) and CHIRPSv2 (0.39) which initially had better performances in the statistical evaluation. Furthermore, the TRMM3B42 Product has previously been found to be inconsistent in mountainous terrains of the tropical region (Ouma et al. 2012) and here; it scored poorer than the other products in the hilly basin 2. At the

slopes of Mt. Elgon, the terrain was found to poorly impact rainfall estimation by most satellite products because of altitude.

The next steps would be to make decisions as to whether and how satellite data should be further processed so that they can be used in conjunction with the gauge data. Preliminary results suggest that they can be used but with slight modifications (Dinku et al. 2018). The real issue is therefore to determine if it is possible to configure a locally robust calibration blueprint that can be applied to the satellite data to ensure that they are compatible with the available gauge data and a calibrated rainfall-runoff model. In this regard, a multi-objective calibration process might be useful for the study area.

The CMORPHv1 product dataset was found to have systemic errors of rainfall estimates in the study area at the daily time-scale, which was compounded in monthly and yearly aggregations and was therefore eliminated from the final analysis in this study.

5 CONCLUSIONS

1. All the products were able to replicate rainfall patterns in space and time, but showed systematic errors in rainfall retrieval that decreased with an increase in rainfall amounts. The systematic errors were mainly in underestimations and showed seasonality, as they were larger during the OND rainy season than during the MAM rainy season. The errors were more evident in a monthly timescale but decreased in a yearly timescale.
2. Products' input data affected their performances in rainfall retrieval. Products using multiple sensors performed better than those with single sensors, especially if the sensors were on different platforms. This increased their ability to retrieve different types of rainfall over SMMRB. This mainly affected TAMSATv2 and PERSIANN-CDR, which use only infrared sensors. A single sensor (infrared) tends to limit rainfall

retrieval ability of different rainfall regimes. The distribution of the rain gauges used in calibration also affects their performance, and thus there is a need to regularly update the algorithms with denser rain gauge data where applicable. This affects the way each product varies in performance from region to region.

3. The satellite products considered are therefore applicable over SMMRB, but errors in high altitude areas need to be considered during the OND season, especially for products using only infrared sensors. To reduce orographic effects, elevation and wind direction data are recommended to be included as input data in the development of algorithms to improve the accuracy of orographic rainfall retrieval.
4. The COSERO hydrological model performance shows quite a good performance in the middle of the basin by most of the products. However, the bias evaluation and the ETA performance indicate that the model attempted to overcompensate for the performance of products such as PERSIANN-CDR and MSWEPv2.2.
5. PERSIANN-CDR was found to overestimate rainfall amounts by up-to 60% and is therefore not ideal for use as an input in hydrological models in the area. CHIRPSv2 and MSWEPv2.2 products perform best with a Correlation coefficient of 0.75 and 0.72, and a Pbias of 14% and 4% respectively. At the lower altitude (Port Victoria Station), all the products were found to overestimate the rainfall amounts.
6. CHIRPSv2 and MSWEPv2.2 were found to be the most suitable products for estimating rainfall amounts in the SMMRB.
7. For the purposes of water resource assessments, the findings indicate that it is crucial to select the SPPs which show good performances in direct comparison with rainfall gauge data and hydrological simulations. Only then can it be used for water resource allocation and planning. The example of CMORPH shows, that one cannot simply use any SPPs but that a careful selection process is necessary.

Acknowledgments: This research is part of the project "Capacity building on the water-energy-food security nexus in Kenya and Uganda" (CAPNEX), project #158 of the Austrian Partnership Programme in Higher Education and Research for Development (APPEAR), funded by the Austrian Development Cooperation (ADC).

Conflicts of Interest: The authors declare no conflict of interest.

REFERENCES

1. Alazzy, A. A., Lü, H., Chen, Abubaker, R., Ali, B., Zhu, Y., and Su, J. (2017). Evaluation of Satellite Precipitation Products and Their Potential Influence on Hydrological Modeling over the Ganzi River Basin of the Tibetan Plateau. *Advances in Meteorology*. https://doi.org/10.1155/2017/3695285.
2. Alemayehu, T., Griensven Av., Senay, G.B., Bauwens, W. (2017). Evapotranspiration Mapping in a Heterogeneous Landscape Using Remote Sensing and Global Weather Datasets: Application to the Mara Basin, East Africa. https://doi.org/10.3390/rs9040390
3. Alfieri, L., Cohen, S., Galantowicz, J., Schimann, G.J-P., Trigg, M.A., Zsoter, E., Prudhomme, C., Kruczkiewicz, A., Perez, E.C. et al. (2013). GloFAS – global ensemble streamflow forecasting and flood early warning. *Hydrology and Earth System Sciences*. doi:10.5194/hess-17-1161-2013
4. Ashouri, H., Hsu, K.L., and Sorooshian, S. (2015). PERSIANNCDR: daily precipitation climate data record from multi-satellite observations for hydrological and climate studies. Bulletin of the *American Meteorological Society*. vol. 96, no. 1, pp. 69–83, 2015. https://doi.org/10.1175/BAMS-D-13-00068.1
5. Awange J. (2021) Improved Remotely Sensed Satellite Products. In: Lake Victoria Monitored from Space. Springer, Cham. https://doi.org/10.1007/978-3-030-60551-3_7
6. Ayanlade, A., Radeny, M., Morton, J.F., and Muchaba, T. (2018). Rainfall variability and drought characteristics in two agro-climatic zones: An assessment of climate change challenges in Africa. https://doi.org/10.1016/j.scitotenv.2018.02.196.
7. Ayugi, B. Tan, G. Ullah, W. Boiyo, R. & Ongoma, V. (2019). Inter-comparison of remotely sensed precipitation datasets over Kenya during 1998–2016. *Atmospheric Research*. https://doi.org/10.1016/j.atmosres.2019.03.032

8. Beck, H.E., A.I.J.M. van Dijk., Wood, E.F., Pan, M., Fisher, C.K., Mirrales, D.G., McVicar, T.R., Adler, R.F. (2019). MSWEP v2 Global 3-hourly 0.1° Precipitation: Methodology and Quantitative Assessment. *Bull. Amer. Meteor. Soc*. https://doi.org/10.1175/BAMS-D-17-0138.1
9. Beck, H.E., Vergopolan, N., Pan, M., Levizzani, V., van Dijk, A.I.J.M., Weedon, G.P., Brocca, L., Pappenberger, F. et al. (2017). Global-scale evaluation of 22 precipitation datasets using gauge observations and hydrological modeling, *Hydrol. Earth Syst. Sci*., 21, 6201-6217, 2017.
10. Belete, M., Deng, J., Wang, K., Zhou, M., Zhu, E., Shifaw, E., Bayissa, Y. (2020). Evaluation of satellite rainfall products for modeling water yield over the source region of Blue Nile Basin. Science of the Total Environment. https://doi.org/10.1016/j.scitotenv.2019.134834
11. Bergström, S. (1995): The HBV model. In: Singh VP (Ed.), Computer Models of Watershed Hydrology. Water Resources Publications, Highland Ranch, CO, USA. pp 443–476.
12. Blöschl, G., Sivapalan, M., Wagener, T., Viglione, A., & Savanije, H. (Eds.). (2013). Runoff prediction in ungauged basins; Synthesis across processes, places and scales. Cambridge. Cambridge University Press.
13. Brocca, L., Massari, C., Pellarin, T. et al. (2020). River flow prediction in data scarce regions: soil moisture integrated satellite rainfall products outperform rain gauge observations in West Africa. Sci Rep 10, 12517 (2020). https://doi.org/10.1038/s41598-020-69343-x
14. Camici, S., Massari, C., Ciabatta, L., Marchesini, I., and Brocca, L. (2020). Which rainfall score is more informative about the performance in river discharge simulation? A comprehensive assessment on 1318 basins over Europe, *Hydrol. Earth Syst. Sci*., 24, 4869–4885, https://doi.org/10.5194/hess-24-4869-2020, 2020.
15. Chen, F., Gao, Y., Wang, Y., Qin, F., & Li, X. (2018). Down-scaling satellite-derived daily precipitation products with an integrated framework. *Intern. J. of Climatology*. https://doi.org/10.1002/joc.5879
16. Coron, L., Andreassian, V., Perrin, C., Lerat, J., Vaze, J., Bourqui, M., Hendrickx, F. (2012). Crash testing hydrological models in contrasted climate conditions: an experiment on 216 Australian catchments. *Water Resources Research*, 48, 5552. doi:10.1029/2011WR011721

17. Chwala, C., & Kunstmann, H. (2019). Commercial microwave link networks for rainfall observation: Assessment of the current status and future challenges. *Wiley Interdiscipl. Rev. Water,* vol. 6, no. 2, pp. e1337, Mar. 2019. https://doi.org/10.1002/wat2.1337
18. Dale, I.R. (1940). The forest types of Mount Elgon. J. East Afr. Uganda Nat. Hist. Soc., 9 (1940), pp. 74-82
19. Dingman, S.L. (2015). *Physical Hydrology* (3rd ed.). Illinois, USA. Waveland Press.
20. Dinku, T., Funk, C., Peterson, P., Maidment, R., Tadesse, T., Gadain, H & Ceccato, P. (2018). Validation of the CHIRPS satellite rainfall estimates over eastern Africa. https://doi.org/10.1002/qj.3244
21. Dinku, T., Ceccato, P. and Connor, S.J. (2011). Challenges to satellite rainfall estimation over mountainous and arid parts of East Africa. *Int. J. Remote Sens*. https://doi.org/10.1080/01431161.2010.499381
22. Duan, Q., Sorooshian, S., Gupta, V.K. (1994). Optimal Use of the SCE-UA Global Optimization Method for Calibrating Watershed Models. *Journal of Hydrology* 158(3-4):265-284 doi: 10.1016/0022-1694(94)90057-4, 1994.
23. Eder, G., Fuchs, M., Nachtnebel H.P., et al. (2005). Semi-distributed modelling of the monthly water balance in an alpine catchment. *Hydrological Processes* 19: 2339-2360. https://doi.org/10.1002/hyp.5888
24. Faramarzi, M., Srinivasan, R., Iravani, M., Bladon, K.D., Abbaspour, K.C., Zehnder, A.J.B., Goss, G.G. (2015). Setting up a hydrological model of Alberta: Data discrimation analyses prior to calibration. https://doi.org/10.1016/j.envsoft.2015.09.006
25. Funk, C., Peterson. P., Landsfeld, M., Pedreros, D., Verdin, J., Shukla, S., Husak, G., Rowland, J., et al (2015). The climate hazards infrared precipitation with stations – a new environmental record for monitoring extremes. *Sci Data* 2, 150066 (2015). https://doi.org/10.1038/sdata.2015.66
26. Gebre, S.L., and Ludwig, F. (2015). Hydrological Response to Climate Change of the Upper Blue Nile River Basin: Based on IPCC Fifth Assessment Report (AR5). *J Climatol Weather Forecasting* 2015, 3:1 http://dx.doi.org/10.4172/2332-2594.1000121
27. Gebrechorkos, S.H., Huelsmann, S., and Bernhofer, C. (2018). Evaluation of multiple climate data sources for managing environmental resources in East Africa. https://doi.org/10.5194/hess-22-4547-2018
28. Habib, E., Elsaadani, M., and Haile A.T. (2012). Climatology-focused Evaluation of CMORPH and TMPA Satellite Rainfall Products over the Nile Basin. *American Meteorological Society*. DOI:10.1175/JAMC-D-11-0252.1

29. Harris, I., Jones, P.D., Osborn, T.J. & Lister, D.H. (2014). Updated high-resolution grids of monthly climatic observations – the CRU TS3.10 Dataset. *International Journal of Climatology, 34*, 623–642. doi.org/10.1002/joc.3711
30. Herrnegger, M., Senoner, T., Nachtnebel, H.P. (2018). Adjustment of spatio-temporal precipitation patterns in a high Alpine environment. *Journal of Hydrology* 556: 913-921. https://doi.org/10.1016/j.jhydrol.2016.04.068
31. Herrnegger M., Nachtnebel, H.P., Schulz, K. (2015). From runoff to rainfall: inverse rainfall–runoff modelling in a high temporal resolution. *Hydrology and Earth System Science* 19: 4619-4639. https://doi.org/10.5194/hess-19-4619-2015
32. Herrnegger, M., Nachtnebel, H.P., Haiden, T. (2012). Evapotranspiration in high alpine catchments - an important part of the water balance! *Hydrology Research* 43: 460. https://doi.org/10.2166/nh.2012.132
33. Huffman, G. J., Bolvin, D. T., Nelkin, E. J., Wolff, D. B.; Adler, R. F., Gu, G., Hong, Y., & Bowman, K. P. (2007). The TRMM Multisatellite Precipitation Analysis (TMPA): Quasi-Global, Multiyear, Combined-Sensor Precipitation Estimates at Fine Scales *Journal of Hydrometeorology, American Meteorological Society.* doi*: https://doi.org/10.1175/JHM560.1*
34. International Union for the Conversation of Nature (IUCN). (2005). Mount Elgon Regional Ecosystem Conservation Programme (MERECP) – Program document. IUCN, Nairobi. http://hdl.handle.net/11671/711
35. Jarvis, A., Reuter, H.I., Nelson, A., Guevara, E. (2008). Hole-filled SRTM for the globe Version 4, available from the CGIAR-CSI SRTM 90m database http://srtm.csi.cgiar.org
36. Jiang, S., Liu, S., Ren, L., Yong, B., Zhang, L., Wang, M., Lu, Y., & He, Y. (2018). Hydrologic Evaluation of Six High Resolution Satellite Precipitation Products in Capturing Extreme Precipitation and Streamflow over a Medium-Sized Basin in China. Water 2018, 10, 25. https://doi.org/10.3390/w10010025
37. Kansiime, K.M., Wambugu, K.S., and Shisanya, A.C. (2013). Perceived and Actual Rainfall Trends and variability in Eastern Uganda: Implications for Community Preparedness and Response. *J. Natural Sci. Res.* http://41.89.10.16/schools/agriculture/images/stories/docs/research/Perceived_and_Actual_Rainfall_Trends_and_Variability.pdf
38. Kimani, M. W., Hoedjes, J.C.B. and Su, Z. (2017). An assessment of satellite-derived rainfall products relative to ground observations over East Africa. *Remote Sens*. 2017, 9, 430; doi:10.3390/rs9050430

39. Kling, H., Stanzel, P., Fuchs, M. et al. (2015). Performance of the COSERO precipitation–runoff model under non-stationary conditions in basins with different climates. *Hydrological Sciences Journal* 60: 1374–1393. https://doi.org/10.1080/02626667.2014.959956
40. Kling, H., Nachtnebel, H.P. (2009). A method for the regional estimation of runoff separation parameters for hydrological modelling. *Journal of Hydrology* 364: 163–174. https://doi.org/10.1016/j.jhydrol.2008.10.015
41. Kling, H. (2002). Development of tools for a semi-distributed runoff model. Diploma thesis, Institute of Water Management, Hydrology and Hydraulic Engineering, University of natural Resources and Applied Life Sciences, Vienna.
42. Knapp, K.R., Ansari, S., Bain, C.L., Bourassa, M.A., Dickinson, M.J., Funk, C., Helms, C.N., Hennon, C.C., Holmes, C.D., Huffman, G.J., et al. (2011). Globally gridded satellite observations for climate studies. *Bull. Am. Meteorol. Soc*. 2011, 92, 893–907.
43. Kratzert, F., Klotz, D., Brenner, C., Schulz, K., and Herrnegger, M.: Rainfall–runoff modelling using Long Short-Term Memory (LSTM) networks. (2018). *Hydrol. Earth Syst. Sci*., 22, 6005–6022. https://doi.org/10.5194/hess-22-6005-2018.
44. Lakew, H.B., Moges, S.A., and Asfaw, D.H. (2020). Hydrological performance evaluation of multiple satellite precipitation products in the upper Blue Nile basin, Ethiopia. https://doi.org/10.1016/j.ejrh.2020.100664
45. Li, L., Hong, Y., Wang, J. et al. (2009). Evaluation of the real-time TRMM-based multi-satellite precipitation analysis for an operational flood prediction system in Nzoia Basin, Lake Victoria, Africa. *Nat Hazards* 50, 109–123 (2009). https://doi.org/10.1007/s11069-008-9324-5
46. Liechti, C. T., Matos, J. P., Boillat, J.-L., and Schleiss, A. J. (2012). Comparison and evaluation of satellite derived precipitation products for hydrological modeling of the Zambezi River Basin, Hydrol. Earth Syst. Sci., 16, 489–500, https://doi.org/10.5194/hess-16-489-2012, 2012.
47. Liu, X., Yang, T., Hsu, K., Liu, C. and S. Sorooshian. (2017). Evaluating the streamflow simulation capability of PERSIANN-CDR daily rainfall products in two river basins on the Tibetan Plateau, *Hydrol. Earth Syst. Sci.,* 21, 169–181, 2017 https://doi.org/10.5194/hess-21-169-2017
48. Ngoma, H., Wen, W., Ojara, M. et al. (2021). Assessing current and future spatiotemporal precipitation variability and trends over Uganda, East Africa, based on

CHIRPS and regional climate model datasets. *Meteorol Atmos Phys* (2021). https://doi.org/10.1007/s00703-021-00784-3

49. Maggioni, V., Massari, C. (2018). On the performance of satellite precipitation products in riverine flood modeling. https://doi.org/10.1016/j.jhydrol.2018.01.039
50. Maidment, R.I., Grimes, D., Black, E., Tarnavsky, E., Young, M., Greatrex, H., Allan, R.P., Stein, T. et al (2017). A new, long-term daily satellite-based rainfall dataset for operational monitoring in Africa. *Sci. Data* 4:170063 doi: 10.1038/sdata.2017.63, 2017.
51. Maidment, R.I., D. Grimes, R.P. Allan, E. Tarnavsky, M. Stringer, T. Hewison, R. Roebeling, and E. Black. (2014). The 30 year TAMSAT African Rainfall Climatology And Time series (TARCAT) data set, J. Geophys. Res. Atmos., 119, 10,619–10,644 doi:10.1002/ 2014JD021927.
52. Mehdi, B., Dekens, J. & Herrnegger, M. (2021). Climatic impacts on water resources in a tropical catchment in Uganda and adaptation measures proposed by resident stakeholders. 2021. *Climatic Change* 164, 10 (2021). https://doi.org/10.1007/s10584-021-02958-9
53. Moriasi, D.N., Arnold, J.G., Van Liew, M.W., Bingner, R.L., Harmel, R.D., and Veith, T.L. (2007). Model evaluation guidelines for systematic quantification of accuracy in watershed simulations. *Transactions of the ASABE*, vol. 50, no. 3, pp. 885–900, 2007.
54. Mugalavai, M. E., Kipjorir, C. E., Raes, D., Rao, S. M. (2008). Analysis of rainfall onset, cessation and length of growing season for western Kenya. https://doi.org/10.1016/j.agrformet.2008.02.013
55. Nachtnebel, H.P, Herrnegger, M., & Senoner, T. (2013). Rainfall – Runoff Model COSERO Handbook. 2013. University of Natural Resources and Life Sciences, Vienna. Department of Water, Atmosphere and Environment, Institute of Hydrology and Water Management (HyWa).
56. Nachtnebel, H.P., Baumung, S., & Lettl, W. (1993). Abflußprognosemodell für das Einzugsgebiet der Enns und der Steyr (in German). Report, Institute of Water Management, Hydrology and Hydraulic Engineering, University of Natural Resources and Applied Life Sciences, Vienna.
57. Nair, A.S., and Indu J. (2017). Performance Assessment of Multi-Source Weighted-Ensemble Precipitation (MSWEP) Product over India. *Climate* 2017, 5, 2; doi:10.3390/cli5010002.
58. Näschen, K., Diekkrüger, B., Leemhuis, C., Steinbach, S., Seregina, L.S., Thonfeld, F., Van der Linden, R. (2018). Hydrological Modeling in Data-Scarce Catchments: The

Kilombero Floodplain in Tanzania. Water 2018, 10, 599. https://doi.org/10.3390/w10050599

59. Oduor, N.O., Ngetich, F.K., Kboi, M.N., Muriuki, A., Adamtey, N., and Mugendi, D.N. (2020). Suitability of different data sources in rainfall pattern characterization in the tropical central highlands of Kenya. https://doi.org/10.1016/j.heliyon.2020.e05375
60. Olang, L. O., Kundu, P. M., Ouma, G., and Furst, J. (2014). Impact of land cover change scenarios on storm runoff generation: a basis for management of the Nyando basin, Kenya, Land Degrad. Dev., 25, 267–277, https://doi.org/10.1002/ldr.2140.
61. Olang, L.O., & Fürst, J. (2010). Effects of land cover change on flood peak discharges and runoff volumes: model estimates for the Nyando River Basin, Kenya. https://doi.org/10.1002/hyp.7821
62. Onyando J. O., Olang L. O., Chemelil M. C. (2005). Regional Analysis of Conceptual Rainfall Runoff Models for Runoff Simulation In Ungauged Catchments: The Case Of Upper Ewaso Ngiro Drainage Basin in Kenya. https://doi.org/10.4314/jcerp.v2i1.29135
63. Ouma, O.Y., Owiti, T., Kipkorir, E., Kibiiy, J., and Tateishi, R. (2012). Multitemporal comparative analysis of TRMM-3B42 satellite-estimated rainfall with surface gauge data at basin scales: daily, decadal and monthly evaluations. *International journal of Remote Sensing*. http://dx.doi.org/10.1080/01431161.2012.701347
64. Pellarin, T., Román-Cascón, C., Baron, C., Bindlish, R., Brocca, L., Camberlin, P., Fernández-Prieto, D., Kerr, Y.H. et al. (2020). The Precipitation Inferred from Soil Moisture (PrISM) Near Real-Time Rainfall Product: Evaluation and Comparison. Remote Sens. 2020, 12, 481. https://doi.org/10.3390/rs12030481
65. Piper, B.S., Plinston, D.T., & Sutcliffe, J.V. (1986). The water balance of Lake Victoria, *Hydrological Sciences Journal*, 31:1, 25-37, DOI: 10.1080/02626668609491025
66. Saha, S., Moorthi, S., Pan, H., Wu, X., Wang, J., Nadiga, S., Tripp, P., Kistler, R., et al. (2010). The NCEP climate forecast system reanalysis. *Bull. Am. Meteorol. Soc*. 2010, 1, 1–146.
67. Schulz, K., Herrnegger, M., Wesemann, J., et al. (2016). Kalibrierung COSERO – Mur für ProVis, Final report. Institute for Water Management, Hydrology and Hydraulic Engineering. University of Natural Resources and Life Science, Vienna, Austria.
68. Sorooshian, S., Hsu, K.L., Gao, X., Gupta, H.V., Imam, B., Braithwaite, D. (2000). Evaluation of PERSIANN system satellite-based estimates of tropical rainfall. *Bull. Am. Meteorol. Soc*. 2000, 81, 2035-2046.

69. Stanzel P, Kahl B, Haberl, U, et al. (2008). Continuous hydrological modelling in the context of real time flood forecasting in alpine Danube tributary catchments. IOP Conference Series: *Earth and Environmental Science* 4: 012005. https://doi.org/10.1088/1755-1307/4/1/012005
70. Stisen, S. & Sandholt, I. (2010). Evaluation of remote-sensing-based rainfall products through predictive capability in hydrological runoff modelling. *Hydrol. Process*. 24(7), 879–891 (2010). https://doi.org/10.1002/hyp.7529.
71. Tarnavsky, E., Grimes, D., Maidment, R., Black, E., Allan, R.P.,and Stringer, M., (2014). Extension of the TAMSAT Satellite-Based Rainfall Monitoring over Africa and from 1983 to Present. https://doi.org/10.1175/JAMC-D-14-0016.1
72. Thiemig, V., Rojas, R., Zambrano-Bigiarini, M., and Roo, De Ad. (2013). Hydrological evaluation of satellite-based rainfall estimates over the Volta and Baro-Akobo Basin. https://doi.org/10.1016/j.jhydrol.2013.07.012
73. Water Resources and Energy Management (WREM), (2008). Sio-Malaba-Malakisi River Basin Monograph.
74. Wesemann, J., Herrnegger, M., Schulz, K. (2018). Hydrological modelling in the anthroposphere: predicting local runoff in a heavily modified high-alpine catchment. J. Mt. Sci. 15: 921. https://doi.org/10.1007/s11629-017-4587-5
75. Williams, K., Chamberlain, J., Buontempo, C., Bain, C. (2015). Regional climate model performance in the Lake Victoria basin. *Clim Dyn* (2015). 44:1699-1713 DOI 10.1007/s00382-014-2201-x
76. Wolski, P., Conradie, S., Jack, C., Tadross, M. (2020). Spatio-temporal patterns of rainfall trends and the 2015–2017 drought over the winter rainfall region of South Africa. International Journal of Climatology. https://doi.org/10.1002/joc.6768
77. Zittis, G. (2018). Observed rainfall trends and precipitation uncertainty in the vicinity of the Mediterranean, Middle East and North Africa. https://doi.org/10.1007/s00704-017-2333-0.

APPENDIX

Table A.1: Calibration values

Calibration (2003 – 2016)		Statistical Measure				
SPP	**Basin**	**NSE**	**PBias**	**MSE (mm)**	**r**	**KGE**
CHIRPS	2	0.3146	0.2834	7.231	0.5699	0.3503
	3	0.362	0.2412	3.4247	0.611	0.4227
	8	0.7183	0.4602	60.1123	0.8488	0.7589
CMORPH	2	0.0845	-0.0702	9.659	0.2985	0.0521
	3	0.2087	0.0581	4.2479	0.4593	0.2056
	8	0.5514	-1.2461	95.7135	0.7795	0.5023
MSWEP	2	0.5613	0.0224	4.6279	0.7554	0.5804
	3	0.3883	0.3062	3.2835	0.6425	0.4139
	8	0.7039	0.1079	63.167	0.8391	0.7755
CDR	2	0.037	-0.0215	10.16	0.259	0.0665
	3	-0.0482	-0.0233	5.6266	0.1111	-0.0972
	8	0.2473	0.8046	160.5898	0.5088	0.3657
TAMSAT	2	0.2726	0.0092	7.6742	0.5221	0.3247
	3	0.1559	0.0555	4.5312	0.3961	0.1592
	8	0.5307	0.4803	100.1282	0.7305	0.5865
TRMM	2	0.341	-0.1286	6.9523	0.5881	0.4556
	3	0.2219	-0.0022	4.177	0.4721	0.2753
	8	0.5407	0.3312	97.9955	0.7366	0.6004

Table A.2: Validation values

Validation (2003 -2016)		Statistical Measure				
SPP	**Basin**	**NSE**	**PBias**	**MSE**	**r**	**KGE**
CHIRPS	2	0.5067	0.2447	4.141	0.7188	0.5615
	3	0.3418	0.0001	5.1507	0.6014	0.46
	8	0.6686	0.3857	46.5056	0.8177	0.7309
CMORPH	2	0.5064	0.2515	4.1503	0.7182	0.5609
	3	0.3567	0.0156	5.1844	0.5974	0.4405
	8	0.6677	0.3942	46.4158	0.8182	0.722
MSWEP	2	0.2275	0.0005	6.4963	0.4772	0.2715
	3	0.3792	0.0465	5.0029	0.6162	0.4663

	8	0.7341	0.4374	37.1437	0.8581	0.7749
CDR	2	0.4648	0.0644	4.5008	0.6883	0.6184
	3	0.3274	0.1791	5.4201	0.577	0.3721
	8	-1.1889	10.063	305.7103	0.2493	-0.0663
TAMSAT	2	0.3363	0.1469	5.5808	0.5861	0.3625
	3	0.3124	-0.0714	5.5413	0.5635	0.4278
	8	0.568	0.3792	60.3352	0.7544	0.6451
TRMM	2	0.5056	0.2567	4.1578	0.7182	0.5562
	3	0.365	-0.0257	5.117	0.606	0.4746
	8	0.6341	0.3079	51.1051	0.7968	0.7045